

Valley Splitting Theory of SiGe/Si/SiGe Quantum Wells

Mark Friesen, Sucismita Chutia, Charles Tahan, and S. N. Coppersmith
*Department of Physics, 1150 University Avenue,
University of Wisconsin-Madison, Madison, WI 53706-1390*

We present an effective mass theory for SiGe/Si/SiGe quantum wells, with an emphasis on calculating the valley splitting. The formalism provides rather simple analytical results for several important problems of physical interest, including a finite square well, a quantum well in an electric field, and a modulation doped two-dimensional electron gas. Of particular importance is the problem of a quantum well at zero magnetic field, grown on a miscut substrate. The latter may pose a numerical challenge for atomistic techniques like tight-binding, because of its two-dimensional nature. In the effective mass theory, however, the results are straightforward and analytical. We compare our various results with those of a tight binding theory, obtaining excellent agreement. The tight binding theory is also used to compute a new effective mass parameter – the valley coupling v_v .

PACS numbers: 73.21.Fg, 78.70.Gq, 78.67.De

I. INTRODUCTION

Silicon heterostructures form the basis of numerous semiconductor technologies. However, state of the art devices are presently so small that further miniaturization must also take into account quantum effects. Of particular interest for silicon are the six quantum states associated with the degenerate valleys in the conduction band structure. Like spins, the valley states may be described by a quantum number. In a quantum well, strain reduces the valley degeneracy to two. The final valley degeneracy is lifted by the singular nature of the quantum well interface, with characteristic energy splittings of order 0.1-1 meV for the case of SiGe/Si/SiGe quantum wells.¹⁻⁶ Because this splitting is comparable in size to the Zeeman splitting, the valley states can compete with spin states for prominence in quantum devices.⁷ For emerging technologies like silicon spintronics⁸ and quantum computing,⁹⁻¹¹ it is therefore crucial to obtain a solid physical understanding of the valley physics, and to develop a predictive theory for the valley states.

The technological significance of valley states was recognized long before the current interest in quantum devices.^{12,13} Early studies focused on bulk silicon, particularly on the electronic states of shallow donors. In this case, valley splitting was known to originate from the singular core of the donor potential, known as the “central cell.”¹⁴ In one theoretical approach, the many-body interactions associated with the central cell were projected onto a single-electron, effective mass (EM) framework, allowing the energy spectrum of the low-lying hydrogenic states to be computed from first principles.¹⁵ Reasonable agreement with experiments was attained. However, because of the complicated projection procedure, a general purpose EM theory was not obtained until more recently.¹⁶

Related techniques were applied to the problem of valley splitting in a semiconductor heterostructure. There were several attempts to develop an EM theory, which is well suited for treating the inhomogeneities occurring in

a quantum well, including conduction band offsets and non-uniform electric fields caused by modulation doping and top-gates. However, the resulting theories proved controversial, and many important valley splitting problems remain unsolved.

Atomistic approaches like tight-binding¹⁷ (TB) have recently enabled new and quantitative tools for calculating the valley splitting. These techniques provide solutions for a range of heterostructure geometries,¹⁷⁻¹⁹ and they offer useful predictions for experiments that prove challenging. For example, oscillations of the valley splitting have been predicted as a function of the quantum well width. These oscillations can be reduced or even eliminated by increasing the electric field. Here, we develop an EM formalism, which reproduces the atomistic results quite accurately, and which provides a simple physical explanation for this intriguing behavior. Specifically, we show that the oscillations occur because of valley coupling interference between the bottom and top interfaces of the quantum well. In an electric field, the wavefunction is squeezed to one side of the quantum well, thereby eliminating the interference effect.

The paper is organized as follows. In Sec. II, we review the two predominant approaches to valley coupling. In Sec. III, we discuss the effective mass theory and we derive the appropriate valley splitting corrections. In Sec. IV, we describe an alternative, tight binding approach, which we use to calculate the new input parameter for the EM theory – the valley coupling v_v – as a function of the conduction band offset ΔE_c . In Sec. V, we apply the EM theory to a finite square well geometry. In Sec. VI, we describe the solution for a quantum well in an external E -field. In Sec. VII, we consider the physically important case of a two-dimensional electron gas (2DEG). In Sec. VIII, we solve the 2D problem of valley splitting at zero field, in a quantum well misaligned with respect to the crystallographic axes. Finally, in Sec. IX, we summarize our results and conclude.

II. EFFECTIVE MASS APPROACH

Earlier EM approaches for valley splitting in a heterostructure include the “electric breakthrough” theory of Ohkawa and Uemura,^{20–22} and the surface scattering theory of Sham and Nakayama.²³ A review of these theories and other related work is given in Ref. [24]. The Ohkawa-Uemura formalism leads to a multi-valley EM theory based on a two-band model involving the lowest two conduction bands at the Γ point of the Brillouin zone, $|\Gamma_1(S)\rangle$ and $|\Gamma_{15}(Z)\rangle$.²⁵ The resulting bulk dispersion relation has a local maximum at the Γ point, and two degenerate valleys, at roughly the correct positions in k -space. The sharp confinement potential at a heterostructure interface provides a natural coupling mechanism for the two z valleys. For an infinite square well of width L , the Ohkawa-Uemura theory obtains a valley splitting of the form $E_v \sim \sin(2k_0L)/L^3$, where $k_0\hat{z}$ is the location of the valley minimum in the Brillouin zone.²² This result was later confirmed by TB theory.^{17,18} The theory therefore captures the main qualitative aspects of the valley physics, with no additional input parameters besides those describing the bulk dispersion relation. In this sense, it is a first principles theory of valley splitting.

However, some aspects of the Ohkawa-Uemura theory have been called into question. First, it has been criticized for its inaccurate description of the dispersion relation near the bottom of the valleys,²⁴ leading to quantitative errors. More importantly, the method relies on a closed EM description, which cannot easily incorporate microscopic details of the quantum well barrier. This contradicts the fact that the valley coupling arises from physics occurring within several angstroms of the interface.²³ Such distances are much smaller than any EM length scale, and cannot be accurately described within any EM theory.

A physically appealing description of the heterostructure interface has been put forward by Sham and Nakayama. These authors construct a basis set of Bloch-like states, which incorporate the reflection, transmission, and valley-scattering of waves at a Si/SiO₂ interface. Since the confinement is built directly into the basis set, it does not appear as an external potential in the envelope equation. Consequently, the envelope equation contains only smooth potentials, which are easily accommodated within the EM approximation. The analytical results for the valley splitting are similar to Ohkawa-Uemura. Indeed, the two approaches have been shown to be closely related.²⁶

The Sham-Nakayama theory has also been criticized. First, the theory is not self-contained, but requires a single unknown input parameter α , characterizing the microscopic width of the interface. Although Sham and Nakayama provide an estimate for α , the parameter is phenomenological. More importantly, the resulting EM theory is somewhat cumbersome, and cannot provide simple analytical solutions for the heterostructure geometries considered here.

Finally, we note that neither the Ohkawa-Uemura theory nor the Sham-Nakayama theory can easily address microscopic deviations from the virtual crystal approximation, which are likely to occur within a unit cell distance from the interface. Because of its sensitivity to physics at the interface, the valley coupling should depend strongly on such microscopic details. An EM formalism that incorporates tunable microscopic parameters is therefore physically motivated.

In this paper, we develop an EM theory which retains the desirable qualities of both the Ohkawa-Uemura and Sham-Nakayama approaches. We introduce a valley coupling parameter v_v , which efficiently describes the valley coupling for any type of interface, and which enables simple analytical results for the valley splitting that are in agreement with atomistic theories.

III. EFFECTIVE MASS THEORY

The EM theory of Kohn and Luttinger¹² forms an excellent description of electrons in a semiconductor matrix under the influence of a slowly varying confinement potential $V(\mathbf{r})$.²⁷ Here, “slowly” is defined with respect to the crystalline unit cell of length a :

$$V(\mathbf{r})/|\nabla V(\mathbf{r})| \gg a. \quad (1)$$

In practice, the EM approach is extremely robust, often proving accurate well outside its range of validity. Indeed, the standard textbook descriptions of shallow donors and quantum wells are both based on the EM theory,²⁷ despite the singular nature of their confinement potentials.

When the validity criterion (1) is not satisfied, it is a good idea to compare the EM results with microscopic or atomistic approaches, such as the TB theory of Sec. IV. For GaAs quantum wells, the EM theory provides quantitatively accurate results in most situations. The approach only breaks down for very narrow quantum wells, or high subband indices.²⁸ On the other hand, for indirect gap semiconductors like silicon, the EM theory must be extended if valley splitting becomes an important issue. A singular confinement potential causes valley coupling, and calls for a more sophisticated treatment. Here, we provide a discussion of both the general multi-valley EM approach, and of the valley coupling, which arises from a sharp quantum barrier.

In the standard EM theory, the wavefunction for a conduction electron in bulk Si can be written as a sum of contributions from the six degenerate valleys. However, the lattice mismatch between Si and Ge in a Si_{1-x}Ge_x/Si/Si_{1-x}Ge_x quantum well causes tensile strain in the Si layer (assuming strain-relaxed SiGe layers). As a result, four of the six valleys rise in energy, while the two z valleys fall in energy.²⁹ The strain splitting is on the order of 200 meV for the composition corresponding to $x = 0.3$.³⁰ Consequently, only z valleys play a role in typical low-temperature experiments.

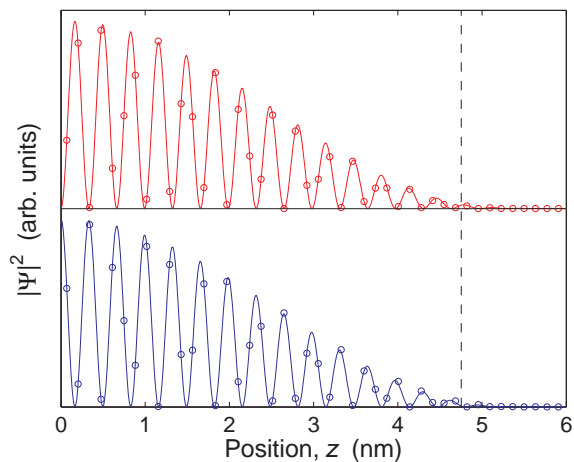


FIG. 1: (Color online.) Comparison of effective mass and tight binding results for the two lowest eigenstates in a $\text{Si}_{0.7}\text{Ge}_{0.3}/\text{Si}/\text{Si}_{0.7}\text{Ge}_{0.3}$ quantum well of width 9.5 nm. (Only half the eigenstate is shown.) The solutions correspond to the same orbital subband, but different valley states. Bottom: ground state. Top: excited state. Solid lines: effective mass theory. Circles: tight-binding theory. Dashed line: quantum well boundary.

The EM wavefunction for strained silicon is then given by

$$\Psi(\mathbf{r}) = \sum_{j=\pm z} \alpha_j e^{ik_j z} u_{\mathbf{k}_j}(\mathbf{r}) F_j(\mathbf{r}). \quad (2)$$

The constants α_j describe the relative phase between the two z valleys, with $|\alpha_{+z}| = |\alpha_{-z}| = 1/\sqrt{2}$. The functions $e^{ik_j z} u_{\mathbf{k}_j}(\mathbf{r})$ are Bloch functions, where $\mathbf{k}_{\pm z} = \pm k_0 \hat{z}$ are the conduction valley minima. The envelope functions $F_j(\mathbf{r})$ are the same for the two z valleys.

A central feature of the EM formalism, which is a consequence of Eq. (1), is that wavefunction separates neatly into atomic scale oscillations (the Bloch functions) and long wavelength modulations (the envelope function). This is demonstrated in Fig. 1, where we show EM and TB results for the two valley states corresponding to the lowest subband of a quantum well, treating the Bloch functions as described in Sec. IV. The two wavefunctions have the same envelope, but their fast oscillations are phase shifted by $\pi/2$. Note that although the EM and TB approaches are fundamentally different (discrete vs. continuous), their wavefunction solutions are almost identical. Also note that the fast oscillations arising from $u_{\mathbf{k}_j}(\mathbf{r})$ (not pictured in Fig. 1) are commensurate with the crystal lattice, while the oscillations from $e^{ik_j z}$ are not, since k_0 is not at the Brillouin zone boundary.

We can draw two main conclusions from the EM/TB comparison. First, the EM treatment correctly captures the essence of the subband physics, including both the long-wavelength and atomic scale features. Higher subbands (not pictured in Fig. 1) are also explained correctly. Second, the main difference between the valley

states does not occur in the envelope function, but in the fast oscillations. To leading order, the valley states are fully characterized by their valley composition vectors $\boldsymbol{\alpha} = (\alpha_{-z}, \alpha_{+z})$. Since the envelope function is independent of the valley physics at this order, the $\boldsymbol{\alpha}$ vectors may be obtained from first-order, degenerate perturbation theory, by treating the valley coupling as a perturbation.³¹ We now describe the perturbation theory, following the approach of Ref. [16], where shallow donors in silicon were considered. We specifically avoid the question of what causes valley splitting, since this lies outside the scope of the EM theory. Instead, we introduce valley coupling phenomenologically, through the parameter v_v .

In the EM formulation of Fritzsche and Tzose,^{32,33} the strained silicon wavefunction, Eq. (2), is determined from the equation

$$0 = \sum_{j=\pm z} \alpha_j e^{-ik_j z} [H_0 + V_v(z) - \epsilon] F_j(z), \quad (3)$$

where

$$H_0 = T(z) + V_{\text{QW}}(z) + V_\phi(z), \quad (4)$$

and

$$T = -\frac{\hbar^2}{2} \frac{\partial}{\partial z} \left(\frac{1}{m_l} \frac{\partial}{\partial z} \right) \quad (5)$$

is the one-dimensional kinetic energy operator. The longitudinal effective mass m_l is materials dependent, and varies from layer to layer in the heterostructure. However, for Si-rich SiGe layers, m_l depends only weakly on the composition. We therefore take $m_l \simeq 0.916m_0$ to be a constant. Note that the transverse effective mass m_t does not appear in Eq. (5), since we initially consider only one-dimensional problems. In Sec. VIII, a more complicated, two-dimensional problem is studied, in which m_t appears.

Three different potential energies appear in Eqs. (3) and (4). $V_{\text{QW}}(z)$ describes the conduction band offsets in the heterostructure. For a quantum well, $V_{\text{QW}}(z)$ corresponds to a pair of step functions. The electrostatic potential energy $V_\phi(z)$ describes any additional, slowly varying potential. Typically, $V_\phi(z) = -eEz$ is an electric field caused by modulation doping in the heterostructure or by external gates.

The EM approximation breaks down near a singular confinement potential like $V_{\text{QW}}(z)$, leading to valley coupling. Very near the singularity, criterion (1) is not satisfied, and it becomes impossible to fully separate the short-wavelength physics of the crystal matrix from the long-wavelength confinement of the excess electron. We can express the missing information in terms of an effective valley coupling potential $V_v(z)$, which vanishes everywhere except within about an atomic length scale from the interface. The detailed form of such a coupling may be quite complicated.¹⁵ However, because it is so strongly peaked, we may treat $V_v(z)$ as a δ -function

over EM length scales. Indeed, the δ -function formulation arises naturally from some first principles theories of valley coupling at heterostructure interfaces.³⁴ We then have

$$V_v(z) = v_v \delta(z - z_i), \quad (6)$$

where z_i is the position of the heterostructure interface along z . In Sec. VIII, we consider a case where z_i depends on position. However in the remainder of the paper, we assume z_i to be constant. The valley interaction potential $V_v(z)$ plays a role analogous to the central cell potential for an electron near a shallow donor.¹⁶ The valley coupling strength v_v is a scalar quantity, which must be determined from experiments, or from atomistic methods like TB.

At lowest order in the perturbation theory (zeroth order), we set $V_v(z) = 0$ in Eq. (3). Because of the fast oscillations associated with the exponential factors, the contributions from the two valleys approximately decouple at this level, reducing Eq. (3) the conventional Kohn-Luttinger envelope equation:

$$\left[-\frac{\hbar^2}{2m_l} \frac{\partial^2}{\partial z^2} + V_{\text{QW}}(z) + V_\phi(z) \right] F^{(0)}(z) = \epsilon^{(0)} F^{(0)}(z), \quad (7)$$

where the superscript (0) denotes an unperturbed eigenstate. Note that the effective mass is the same for the two z valleys. The corresponding envelopes are therefore equal, and we shall drop the valley index.

We now solve for α and ϵ in Eq. (3) using first order perturbation theory. By replacing $F_j(z)$ in Eq. (3) with its zeroth order approximation, left-multiplying by $F^{(0)*}(z)e^{ik_l z}$, and integrating over z , we can express Eq. (3) in matrix form:

$$\begin{pmatrix} \epsilon^{(0)} + \Delta_0 & \Delta_1 \\ \Delta_1^* & \epsilon^{(0)} + \Delta_0 \end{pmatrix} \begin{pmatrix} \alpha_{-z} \\ \alpha_{+z} \end{pmatrix} = \epsilon \begin{pmatrix} \alpha_{-z} \\ \alpha_{+z} \end{pmatrix}. \quad (8)$$

We have dropped small terms containing atomic scale oscillations in the integrand. The perturbation terms are defined as follows:

$$\Delta_0 = \int V_v(z) |F^{(0)}(z)|^2 dz, \quad (9)$$

$$\Delta_1 = \int e^{-2ik_0 z} V_v(z) |F^{(0)}(z)|^2 dz. \quad (10)$$

Diagonalizing Eq. (8) gives the first order energy eigenvalues

$$\epsilon_\pm = \epsilon^{(0)} + \Delta_0 \pm |\Delta_1|. \quad (11)$$

The valley splitting is given by

$$E_v = 2|\Delta_1|. \quad (12)$$

In the valley basis $(\alpha_{-z}, \alpha_{+z})$, the eigenvectors corresponding to ϵ_\pm are given by

$$\alpha_\pm = \frac{1}{\sqrt{2}} \left(e^{i\theta/2}, \pm e^{-i\theta/2} \right). \quad (13)$$

Here, \pm refers to the even or odd valley combinations, and we have defined the phases

$$e^{i\theta} \equiv \Delta_1 / |\Delta_1|. \quad (14)$$

For the case of a single interface at $z = z_i$, we obtain

$$\Delta_0 = v_v |F^{(0)}(z_i)|^2, \quad \Delta_1 = v_v e^{-2ik_0 z_i} |F^{(0)}(z_i)|^2. \quad (15)$$

We see that it is the magnitude of the envelope function at the interface that determines the strength of the valley coupling. The resulting α_\pm vectors are determined by

$$\theta = 2k_0 z_i. \quad (16)$$

The valley coupling integrals in Eqs. (9) and (10) provide a simple but efficient characterization of the valley splitting. The coupling parameter v_v , which is yet to be determined, provides a means to incorporate important microscopic details about the interface. The utility of the present theory can be seen in the simplicity of the results obtained in the following sections. The accuracy of the theory can be seen in the agreement between the EM and TB techniques.

We close this section by noting that several authors have criticized the Fritzsche-Twose formulation of the multi-valley EM theory,^{24,35} particularly because of the way intervalley kinetic energy terms are calculated.²⁰ However, we emphasize that the present treatment includes all first order corrections to the valley splitting. Since the intervalley kinetic energy is of order v_v^2 , it has a weaker contribution. The previous criticisms therefore do not apply here.

IV. TIGHT-BINDING THEORY

We now discuss a tight binding method for modeling heterostructures in silicon. Our main goal is to compare the solutions from such an atomistic technique with those of the EM theory, and to compute the valley coupling parameter v_v , whose value cannot be determined within the present EM theory. We focus on the two-band TB model of Boykin *et al.*,^{17,18} because of its simplicity.

In the two-band model, the TB Hamiltonian includes nearest neighbor and next-nearest neighbor tunnel couplings, v and u , respectively. The values $v = 0.683$ eV and $u = 0.612$ eV are chosen such that (i) the bulk dispersion relation $\epsilon(k)$ has two valleys, centered at $|k| = k_0 = 0.82 \cdot 2\pi/a$, and (ii) the curvature of $\epsilon(k)$ at the bottom of a valley gives the correct longitudinal effective mass $m_l = 0.916m_0$. The unit cell in this theory consists of two atoms, with separation $a/4$ along the [001] axis, where $a = 5.431$ Å is the length of the silicon cubic unit cell. These parameters correspond to bulk silicon. A more sophisticated theory should take into account compositional variations and strain conditions. However, for most situations of interest, the modified parameters differ only slightly from the bulk.

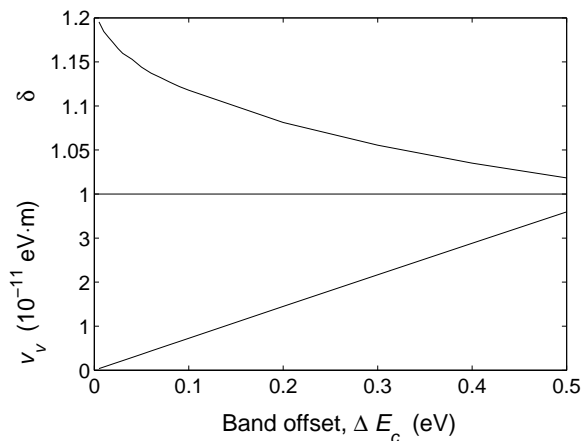


FIG. 2: The valley coupling parameter v_v and the quantum well parameter δ , defined in Eq. (27), as a function of the conduction band offset ΔE_c . The results are obtained for a symmetric, finite square well by comparing the EM and TB theories.

In addition to the tunnel couplings v and u , we can also include onsite parameters λ_i , to provide a locally varying confinement potential. Both the conduction band offset $V_{\text{QW}}(z)$ and the electrostatic potential $V_\phi(z)$ can be expressed as on-site terms. To avoid boundary errors, we choose a TB lattice much larger than the confined electronic wavefunction. Diagonalization of the resulting TB Hamiltonian gives energy eigenvalues, from which we can calculate the valley splitting.

The two-band TB theory describes silicon valley physics with a minimal number (2) of input parameters. More sophisticated techniques can provide numerical improvements, but they generally do not capture any new physics. In Ref. [17], a comparison of the valley splitting between the two-band theory and a detailed many-band theory shows excellent qualitative agreement. The more accurate treatment gives results that are smaller by an approximately constant factor of 25%.

Some typical TB eigenstates for a finite square well are shown in Fig. 1. The data points correspond to the squared TB amplitudes plotted at the atomic sites. Comparison with the full EM wavefunctions requires knowledge of the Bloch functions in Eq. (2). However, to make contact with the TB results, we only need to evaluate the Bloch functions at the atomic sites. According to Eq. (2) and Sec. V, the two low-lying EM wavefunctions can be expressed as

$$\Psi_\pm(z) = \frac{1}{\sqrt{2}} [u_{-k_0}(\mathbf{r})e^{-ik_0z} \pm u_{+k_0}(\mathbf{r})e^{+ik_0z}] F(z), \quad (17)$$

where the ground-state alternates between $+$ and $-$ as a function of L . We can denote the two atoms in the TB unit cell as A and B , with the corresponding Bloch functions $u_{k_0}(A)$ and $u_{k_0}(B)$. By translational symmetry, we must have $|u_{k_0}(A)| = |u_{k_0}(B)|$. [Our TB calculations suggest that $u_{k_0}(A) = -u_{k_0}(B)$.] The Bloch func-

tions satisfy time-reversal symmetry, so that $u_{k_0}^*(\mathbf{r}) = u_{-k_0}(\mathbf{r})$. Thus, defining $u_{k_0}(A) = |u_{k_0}(A)|e^{i\varphi}$ and assuming proper normalization, we find that the squared TB amplitudes should fall on the curves

$$|\Psi_+(z)|^2 = 2 \cos^2(k_0z + \varphi) F^2(z) \quad (18)$$

$$|\Psi_-(z)|^2 = 2 \sin^2(k_0z + \varphi) F^2(z), \quad (19)$$

where all information about the Bloch functions is reduced to the unimportant phase variable φ . Eqs. (18) and (19) are plotted in Fig. 1, setting $\varphi = 0$. We see that these analytical forms provide an excellent representation of the TB results. However, we emphasize that Eqs. (18) and (19) are accurate only at the atomic sites. To describe the wavefunction between the atomic sites would require additional knowledge of the silicon Bloch functions.³⁶⁻³⁹

We can use the TB theory to determine the EM valley coupling parameter v_v by comparing corresponding results in the two theories. This is accomplished in Sec. V for the finite square well geometry, with results shown in Fig. 2.

V. FINITE SQUARE WELL

We consider a symmetric square well with barrier interfaces at $z_i = \pm L/2$, corresponding to a quantum well of width L . We assume that the two interfaces are equivalent, so the same valley coupling v_v can be used on either side. The resulting valley splitting is

$$E_v = 4v_v F^2(L/2) |\cos(k_0L)|. \quad (20)$$

An analytical solution for the envelope function of a finite square well can be obtained by matching wavefunction solutions at the interfaces,²⁷ giving

$$F(L/2) = \left[\frac{1}{k_b} + \frac{k_w L + \sin(k_w L)}{2k_w \cos^2(k_w L/2)} \right]^{-1/2}, \quad (21)$$

where

$$k_b = k_w \tan(k_w L/2). \quad (22)$$

The wavevector k_w may be obtained numerically from the following transcendental equation:

$$k_w^2 = \frac{2m_l \Delta E_c}{\hbar^2} \cos^2(k_w L/2). \quad (23)$$

Typical results for the valley splitting as a function of well width are shown in Fig. 3.

An approximate solution for Eqs. (20)-(23) can be obtained in the limit of a very deep or a very wide quantum well. When $\pi^2 \hbar^2 / 2m_l L^2 \ll \Delta E_c$, we find that $k_w \simeq \pi/L$ for the first subband, leading to

$$F^2(L/2) \simeq \frac{\pi^2 \hbar^2}{m_l \Delta E_c L^3}. \quad (24)$$

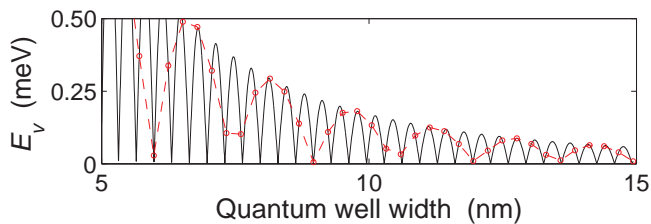


FIG. 3: (Color online.) Valley splitting in a finite square well. We compare effective mass results (solid curve) with tight binding results (circles), as a function of the quantum well widths L and L' , respectively (see text). The TB data points occur in discrete increments of the well width, corresponding to a TB unit cell. We assume a $\text{Si}_{0.7}\text{Ge}_{0.3}/\text{Si}/\text{Si}_{0.7}\text{Ge}_{0.3}$ quantum well, corresponding to $\Delta E_c = 160$ meV.

The valley splitting is then given by

$$E_v \simeq \frac{4v_v\pi^2\hbar^2}{m_l\Delta E_c L^3} |\cos(k_0 L)|. \quad (25)$$

This agrees with the L dependence obtained in Refs. [17] and [22] for an infinite square well.

Diagonalization of the perturbation Hamiltonian in Eq. (8) also gives the ground (g) and excited (x) valley state α vectors

$$\begin{aligned} \alpha_g &= (1, -\text{sign}[\cos(k_0 L)])/\sqrt{2} && \text{(ground)}, \\ \alpha_x &= (1, \text{sign}[\cos(k_0 L)])/\sqrt{2} && \text{(excited)}, \end{aligned} \quad (26)$$

where we have defined $\text{sign}[x] \equiv x/|x|$. These results are equivalent to Eq. (13), up to an overall phase factor. We see that the oscillations in Fig. 3 correspond to alternating even and odd ground states [$\alpha_+ = (1, 1)/\sqrt{2}$ and $\alpha_- = (1, -1)/\sqrt{2}$, respectively], as a function of L . The alternating behavior has been observed previously in TB analyses.¹⁷

We can use these results to obtain an estimate for the valley coupling parameter v_v , by comparing the EM and TB results for a finite square well. For the EM case, we first solve Eq. (23) numerically, to obtain k_w . We then solve Eq. (21) for $F(L/2)$, finally obtaining the valley splitting from Eq. (20). For a given value of ΔE_c , we fit Eq. (20) to the numerical TB results, as a function of L , using v_v as a fitting parameter. However, there is an ambiguity in relating the quantum well width, L , in the continuous EM theory to the discretized width, $L' = Na/2$, in the TB theory, where N is the number of silicon TB unit cells in the quantum well. For example, is the interface located on the last Si atomic site of the quantum well, the first Ge atomic site of the barrier, or somewhere in between? We see that the two widths, L and L' , may differ on the order of a single atomic layer, $a/4 = 1.36$ Å. To allow for this, we introduce a second fitting parameter δ , as defined in

$$L = L' + \delta a/4. \quad (27)$$

With these two fitting parameters, v_v and δ , we obtain

nearly perfect correspondence between the EM and TB theories, as shown in Fig. 3.

In this manner, we can map out v_v and δ as a function of ΔE_c , giving the results shown in Fig. 2. We find that $v_v(\Delta E_c)$ is linear over its entire range, with

$$v_v = 7.2 \times 10^{-11} \Delta E_c. \quad (28)$$

Here, v_v is given in units of eV·m when ΔE_c is expressed in units of eV. As described in Sec. IV, a many-band TB analysis would obtain results for v_v that are smaller by a factor of about 25%.

From Fig. 2, we see that $\delta \simeq 1.1$ forms a reasonable approximation over the typical experimental range of ΔE_c (50-200 meV). This corresponds to about one atomic layer, or half an atomic layer on either side of the quantum well. We can interpret δ as the set-back distance for an effective scattering barrier which causes valley coupling. A similar interpretation was given for the parameter α in Ref. [23]. We see that this set-back distance increases for shallow quantum wells. We shall give a theoretical explanation for this behavior elsewhere.

Finally, we consider the asymptotic limits of our EM theory. In the limit $\Delta E_c \rightarrow \infty$, corresponding to an infinite square well, Eq. (25) becomes exact. Since E_v does not vanish, we conclude that $v_v \propto \Delta E_c$ in this limit. This is precisely the behavior observed in Fig. 2.

In the limit $\Delta E_c \rightarrow 0$, corresponding to a shallow square well, Eq. (25) is not valid. Instead, we obtain $F^2(L/2) \simeq \Delta E_c L m_l / \hbar^2$, leading to $E_v \simeq 2\Delta E_c L v_v m_l \cos(k_0 L) / \hbar^2$. In this limit, we expect the valley splitting to vanish, but we can make no other predictions about v_v . The numerical results, however, suggest that the linear dependence of $v_v(\Delta E_c)$ extends smoothly to zero.

VI. QUANTUM WELL IN AN ELECTRIC FIELD

We now consider a quantum well, with an electric field oriented in the growth direction. The geometry is shown in the inset of Fig. 4. For physically realistic fields due to modulation doping or electrical top-gates, the electrostatic potential varies slowly according to criterion (1). Thus, we may treat the quantum well interface as in Sec. V, using the numerical values for $v_v(\Delta E_c)$, obtained in a symmetric square well. The electrostatic potential enters our analysis through the envelope equation (8). There are no exact solutions for the problem of a tilted square well. However, the approximate treatment described here provides analytic results that agree well with the TB theory.

We assume an electrostatic potential given by $V_\phi(z) = -eEz$, and a quantum well of width L and height ΔE_c . The top barrier of the well lies at $z = 0$. We

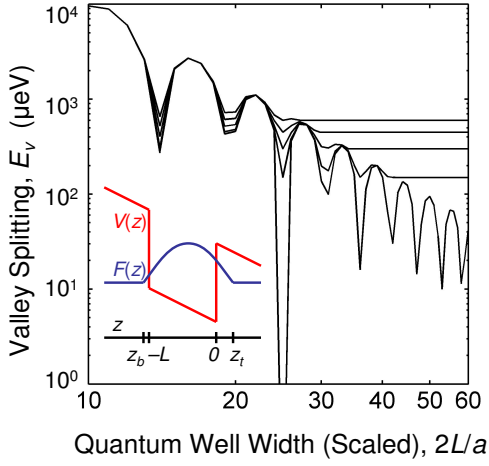


FIG. 4: (Color online.) Effective mass results for the valley splitting in an electric field, as a function of the quantum well width. Five E fields are shown, from bottom to top: $E = 0, 1.04, 2.08, 3.12,$ and 4.16 MV/m. The well width L is scaled by the TB unit cell size, $a/2 = 2.716$ Å. Results are shown for a $\text{Si}_{0.8}\text{Ge}_{0.2}/\text{Si}/\text{Si}_{0.8}\text{Ge}_{0.2}$ quantum well, analogous to Fig. 1(a) of Ref. [17]. Inset: E -field geometry, with confinement potential $V(z) = V_{\text{QW}}(z) + V_{\phi}(z)$ and variational wavefunction $F(z)$ given in Eq. (29). Here, $z_b = z_t - \pi/k$.

consider the following variational envelope function:

$$F(z) = \begin{cases} -\sqrt{\frac{2k}{\pi}} \sin[k(z - z_t)] & (z_t - \frac{\pi}{k} < z < z_t) \\ 0 & (\text{otherwise}). \end{cases} \quad (29)$$

For simplicity, we have chosen a wavefunction tail that terminates abruptly. This approximation is satisfactory for a variational calculation, since the exponentially suppressed tail contributes very little to the energy expectation value.

In our trial function, the parameter k accounts for the finite barrier height by allowing the wavefunction to extend into the barrier region. The upward shift of the wavefunction in the presence of an electric field is given by z_t . Eq. (29) becomes the exact solution for an infinite square well when $\Delta E_c \gg 1$, suggesting that the trial function will be most effective in this limit. We therefore define the small parameters

$$x = \frac{\hbar^2 \pi^2}{2m_i L^2 \Delta E_c} \quad \text{and} \quad y = \frac{eEL}{4\Delta E_c}. \quad (30)$$

The energy expectation value, obtained from envelope equation (2), can be expressed in terms of the dimensionless variational parameters

$$\theta_1 = kL \quad \text{and} \quad \theta_2 = kz_t, \quad (31)$$

giving

$$\frac{\pi^2 \epsilon}{\Delta E_c} \simeq \begin{cases} x\theta_1^2 - 4\pi^2 y(\theta_2 - \pi/2)/\theta_1 + 2\pi[\theta_2^3 - (\theta_1 + \theta_2 - \pi)^3]/3 & (\theta_1 + \theta_2 < \pi) \\ x\theta_1^2 - 4\pi^2 y(\theta_2 - \pi/2)/\theta_1 + 2\pi\theta_2^3/3 & (\theta_1 + \theta_2 \geq \pi). \end{cases} \quad (32)$$

The first case corresponds to the penetration of the wavefunction into the bottom barrier. For large enough electric fields ($y > x$), this penetration ceases, and there is no contribution from the bottom barrier. (See inset of Fig. 4.) Minimization of ϵ with respect to θ_1 and θ_2 gives

$$\left. \begin{aligned} \theta_1 &\simeq \pi + \sqrt{x-y} - \sqrt{x+y} \\ \theta_2 &\simeq \sqrt{x+y} \end{aligned} \right\} \quad (x > y), \quad (33)$$

$$\left. \begin{aligned} \theta_1 &\simeq \pi(y/x)^{1/3} \\ \theta_2 &\simeq (8y^2x)^{1/6} \end{aligned} \right\} \quad (x \leq y), \quad (34)$$

where we have made use of the fact that $\theta_2 \ll \pi$. For the case $x > y$, we have also used $\pi - \theta_1 \ll \pi$.

To compute the valley splitting, we use the results $F^2(-L) \simeq 2(\pi - \theta_1 - \theta_2)^2/L$ and $F^2(0) \simeq 2\theta_2^2/L$ when

$x > y$, and $F^2(0) \simeq 2\theta_2^2\theta_1/\pi L$ when $x \leq y$ to obtain

$$E_v L \simeq \begin{cases} 4v_v |e^{ik_0 L}(x-y) + e^{-ik_0 L}(x+y)| & (x > y) \\ 8v_v y & (x \leq y). \end{cases} \quad (35)$$

These solutions are plotted in Fig. 4 as a function of the quantum well width for several different E fields. In the figure, we have evaluated Eq. (35) only at discrete increments of a TB unit cell, to facilitate comparison with Fig. 1(a) in Ref. [17]. The correspondence between the EM and TB theories is quantitatively and qualitatively accurate, particularly for large well widths.

In Fig. 4, we see that the crossover to high field behavior corresponds to E_v becoming independent of L . The crossover occurs when $y > x$ or

$$E > \frac{2\pi^2 \hbar^2}{m_i e L^3}. \quad (36)$$

At low fields, the valley splitting exhibits interference oscillations, similar to Fig. 3. At high fields, the envelope function no longer penetrates the barrier on the bottom side of the quantum well. The top and bottom barriers then no longer produce interfering contributions to the valley splitting, causing the oscillations in $E_v(L)$ to cease. Since we have chosen a trial wavefunction with no tail, the crossover to high field behavior in Fig. 4 occurs abruptly. This is in contrast with the TB results where small oscillations can still be observed right above the crossover.

In the zero field limit $y \rightarrow 0$, Eq. (35) reduces correctly to Eq. (25) for a symmetric square well. In the high field limit, we can ignore the bottom barrier entirely. For the case of an infinite barrier, the high field limit is often studied using the Fang-Howard trial wavefunction.²⁷ However for a finite barrier, we obtain a more accurate result by allowing the Fang-Howard function to penetrate the top barrier, similar to Eq. (29). Indeed, it is the value of the wavefunction at the barrier which determines the valley splitting. An appropriately modified trial function is given by

$$F(z) = \begin{cases} -\sqrt{b^3/2}(z - z_t) \exp[b(z - z_t)/2] & \text{for } z < z_t \\ 0 & \text{for } z \geq z_t \end{cases}. \quad (37)$$

This is just the usual Fang-Howard variational function, shifted upward by z_t . The wavefunction tail decays exponentially into the lower portion of the quantum well. The exponential suppression of the tail is more accurate than the abrupt termination assumed in Eq. (29), although an exact treatment of the triangular well shows that the asymptotic behavior of the Fang-Howard trial function is still incorrect.²⁷ Following the conventional Fang-Howard approach, and using both b and z_t as variational parameters, we obtain

$$E_v = \frac{2v_v eE}{\Delta E_c}. \quad (38)$$

As in the case of a symmetric square well, we see that $E_v \propto \Delta E_c^{-1}$. We also see that Eq. (38) is identical to the high-field limit of Eq. (35). Thus, the non-oscillating, high-field portions of the curves in Fig. 4 correspond to the ‘‘Fang-Howard limit’’ described by Eqs. (37) and (38). This agreement demonstrates that the variational form of Eq. (29) is robust over the entire field range.

VII. VALLEY SPLITTING IN A 2DEG

The EM theory is well suited for treating many-body problems, such as the two dimensional electron gas (2DEG) in a SiGe/Si/SiGe quantum well. We consider the modulation-doped heterostructure shown in Fig. 5(a). In this structure, we assume that the charge is found only in the 2DEG and the doping layers. A more detailed analysis could also include background charge and charge trapped at an interface. The conduction band

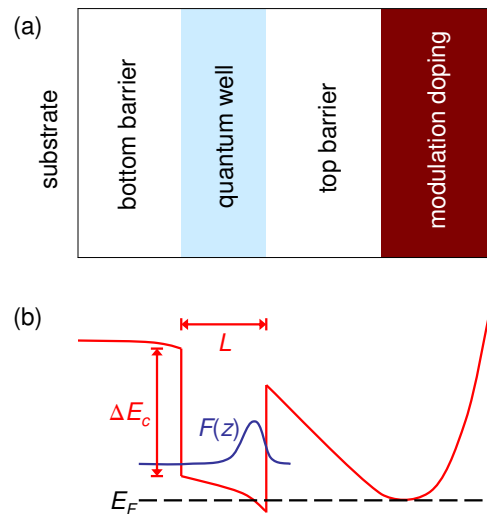


FIG. 5: (Color online.) Typical 2DEG structure for a SiGe/Si/SiGe quantum well. (a) Heterostructure, left to right: strain-relaxed SiGe substrate and barrier, strained silicon quantum well, strain-relaxed SiGe barrier, n^+ SiGe doping layer. (b) Conduction band profile, showing the envelope function $F(z)$ and the Fermi energy E_F .

profile is sketched in Fig. 5(b). We treat the many-body interactions, here, by means of the Hartree approximation, although more accurate approximations can also be used. Because the modulation doping field is usually large in a realistic heterostructure, we will ignore the bottom barrier in our calculations.

The modified Fang-Howard trial wavefunction of Eq. (37) gives a reasonable approximation for an electron in a 2DEG.¹³ However, we must include the electron-electron interactions self-consistently. Within the Hartree approximation,²⁷ the 2DEG charge density $\rho(z)$ is given by

$$\rho(z) = -enF^2(z), \quad (39)$$

where n is the density of the 2DEG. The charge density is related to the electrostatic potential through the Poisson equation,

$$\frac{d^2 \phi_H}{dz^2} = -\frac{\rho}{\varepsilon}, \quad (40)$$

where ε is the dielectric constant for silicon. The boundary conditions on Eq. (40) are given by

$$\begin{aligned} d\phi_H/dz &= 0 & (z \rightarrow -\infty), \\ \phi_H &= 0 & (z = 0). \end{aligned} \quad (41)$$

The second boundary condition anchors the energy of the confinement potential, $V_{QW}(z)$, at top of the quantum well.²⁷ The corresponding electrostatic potential is given by

$$\begin{aligned} \phi_H(z) = \frac{en}{2b\varepsilon} \left\{ [b^2(z - z_t)^2 - 4b(z - z_t) + 6]e^{b(z - z_t)} \right. \\ \left. - [b^2 z_t^2 + 4bz_t + 6]e^{-bz_t} \right\} \end{aligned} \quad (42)$$

The variational parameters are determined by minimizing the total energy per electron,

$$\epsilon = \langle T \rangle + \frac{1}{2} \langle V_\phi \rangle + \langle V_{\text{QW}} \rangle, \quad (43)$$

Here, $V_\phi(z)$ corresponds to the Hartree potential $-e\phi_H(z)$. The factor of 1/2 in this term prevents overcounting of the interactions.²⁷ Note that, in contrast with calculations for Si/SiO₂ inversion layers, we do not include any contributions from image potentials in Eq. (43), since the dielectric constants for Si and SiGe are nearly equal, and any other interfaces that could produce images are far away from the 2DEG.

We evaluate Eq. (43), obtaining

$$\epsilon \simeq \frac{\hbar^2 b^2}{8m_l} + \frac{e^2 n}{4b\epsilon} \left(\frac{33}{8} - 2bz_t \right) + \frac{\Delta E_c b^3 z_t^3}{6}, \quad (44)$$

where we have made use of the dimensionless small parameters bz_t and $e^2 n / \epsilon \Delta E_c b$. The first of these describes the shift of the wavefunction towards $+\hat{z}$, while the second describes the relative magnitude of the electrostatic energy with respect to the band offset ΔE_c . Minimization of ϵ with respect to b and z_t gives

$$z_t^2 \simeq \frac{8\hbar^2}{33m_l \Delta E_c} \quad \text{and} \quad b^3 \simeq \frac{33e^2 n m_l}{8\hbar^2}. \quad (45)$$

We can now calculate the valley splitting for a 2DEG. Under the previous approximations, we obtain a very simple expression for the wavefunction at the top quantum well interface,

$$F^2(0) \simeq \frac{e^2}{2\epsilon \Delta E_c}, \quad (46)$$

giving the valley splitting

$$E_v = \frac{v_v e^2 n}{\epsilon \Delta E_c}. \quad (47)$$

This result assumes a perfectly smooth interface. As we show in Sec. VIII, substrate roughness can reduce this estimate significantly. However, the suppression is due to geometrical effects, so the scaling dependence in Eq. (47) should remain valid.

We can use our numerical results for the valley coupling parameter in Eq. (28) to obtain a quantitative estimate for the valley splitting in a 2DEG. Expressing the valley splitting in units of meV and the 2DEG density n in units of 10^{12} cm^{-2} , we find that

$$E_v \simeq 1.14n, \quad (48)$$

where we have assumed the low-temperature dielectric constant for silicon, $\epsilon = 11.4\epsilon_0$. It is interesting to note that the barrier height ΔE_c does not directly enter this result.

In Eq. (48), the prefactor 1.14 can be compared with similar estimates for silicon inversion layers. Ohkawa and

Uemura obtain a prefactor of 0.15,^{20,21} while Sham and Nakayama obtain 0.33.⁴⁰ A recent experiment in a top-gated SiO₂/Si/SiO₂ heterostructure has obtained a much larger value of the valley splitting.⁴¹ However, several remarks are in order. First, we do not specifically consider top-gated structures here, so Eq. (48) does not directly apply to the latter experiment. Second, we point out that depletion and image charges, which were not considered here, play a more significant role for inversion layers as compared to quantum wells. Finally, as discussed above, we note that a more accurate many-band estimate for v_v would reduce the estimate in Eq. (48) by about 25%.

VIII. TILTED QUANTUM WELL AT $B = 0$

While TB theories have proven successful for studying valley splitting in simple geometries, there is an obvious scaling problem when we extend these techniques to higher dimensions. For high-dimensional problems, the EM theory of valley splitting has a definite, practical advantage.

Here, we consider the important and physically realistic 2D geometry of a quantum well tilted with respect to the crystallographic axes, as shown in Fig. 6. In high-mobility Si/SiGe devices, substrates are often intentionally tilted away from [001] by up to several degrees, to promote uniform epitaxial growth under strain conditions, and to help reduce step bunching. However, some amount of growth disorder always persists in conventional strained devices. (Recent advances in nanomembrane technology may help overcome this difficulty.⁴²) Typical devices therefore contain atomic steps at their surfaces and interfaces, as consistent with local or global tilting. At the EM level, one might expect to ignore such small (atomic) steps, and to work, at least locally, in the tilted basis (x', y', z') shown in Fig. 6. However, when valley coupling is taken into account, the problem becomes two-dimensional, since the tilted surface is misaligned with respect to the crystallographic axes.

We consider a tilted quantum well at zero magnetic field. (Non-zero fields are considered elsewhere.^{26,43}) At zero field, the electronic wavefunction extends over an infinite number of steps. Under such conditions, we expect a strong suppression of the valley splitting. To see this, we note that the position of the interface $z_i(x)$ in Eq. (6) becomes a function of the lateral position, so the phase factor in Eq. (10) is no longer a constant. The resulting interference effects are similar to the valley splitting interference between the top and bottom interfaces of a quantum well, studied in Sec. V. However, in the present case, every step contributes to the interference with a different phase, resulting in a complete suppression of the valley splitting.⁴³ On the other hand, the experimental data suggest a small, but nonzero valley splitting at zero field.⁶ To explain this behavior, we note that the phase factor $e^{i2k_0 z}$ in Eq. (10) oscillates as a function of position along \hat{z} , with period π/k_0 . But the phase factor is

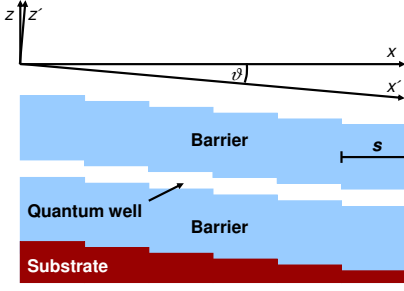


FIG. 6: (Color online.) Tilted quantum well geometry, with crystallographic axes (x, y, z) and rotated axes (x', y', z') , assuming $y = y'$. The effective tilt angle is φ , and the atomic step size is s .

evaluated at different positions along the tilted interface. As a function of position along \hat{x} , the phase has period $\pi/k_0 \sin \vartheta \simeq \pi/k_0 \vartheta$, where ϑ is the tilt angle. If wavefunction oscillations were present, with this same period, they would naturally induce a valley splitting. Therefore, if the kinetic energy cost of such oscillations is not prohibitive, they will arise spontaneously, in order to lower the electronic energy. We now determine the magnitude of these charge oscillations by assuming a trial wavefunction and minimizing the total energy.

We first express the envelope equation in the tilted basis (x', y', z') , giving

$$\left[\sum_{n=1}^3 \frac{1}{2m_n} \left(-i\hbar \frac{\partial}{\partial x'_n} + eA_n(\mathbf{r}') \right)^2 + V_{\text{QW}}(z') \right] F(\mathbf{r}') = \epsilon^{(0)} F(\mathbf{r}'), \quad (49)$$

where $m_1 = m_2 = m_t = 0.191 m_0$ and $m_3 = m_l = 0.916 m_0$, are the transverse and lateral effective masses, respectively.⁴⁴ We have included a vector potential $\mathbf{A}(\mathbf{r}') = (0, Bx', 0)$ in Eq. (49), for generality, although we will eventually take the limit $B \rightarrow 0$. We now introduce the valley coupling as a perturbative correction to $\epsilon^{(0)}$, given by

$$\epsilon_v = |\Delta_1| = \int e^{-i2k_0(z' - x'\vartheta)} V_v(z') |F(\mathbf{r}')|^2 dx' dz'. \quad (50)$$

Here, the valley coupling potential is given by $V_v(z') = v_v \delta(z')$, where we take $z' = 0$ to be the top of the quantum well (the location of the two dimensional electron gas).

For completeness, we also include a second energy correction

$$\epsilon_s = \int V_s(x') |F(\mathbf{r}')|^2 dx' dz', \quad (51)$$

arising from the “washboard” potential $V_s(x') = -v_s \cos(k_s x')$, which approximates the periodic thickness variations of the quantum well, due to atomic steps at the

interface. Here, $k_s = 2\pi/s$, where s is the step width. The amplitude of the washboard potential v_s is small for the case of a wide quantum well. The effect of the washboard potential is to induce charge oscillations of wavevector k_s , which are commensurate with the steps. In contrast, the valley potential V_v induces incommensurate oscillations of wavevector $2k_0\vartheta$. The ratio of the two wavevectors is a constant, with $k_s/2k_0\vartheta = 2.35$ for silicon.

We now consider a trial wavefunction of the form $F(\mathbf{r}') = F_{xy}(x', y') F_z(z')$. There is an exact solution for $F_{xy}(x', y')$ in the unperturbed envelope equation (49), given by²⁷

$$f_{nk}(x', y') \sim H_{n-1}[(x' - x_k)/l_B] e^{iky'} e^{-(x' - x_k)^2/2l_B^2} \quad (52)$$

where $H_n(x)$ is a Hermite polynomial and $x_k = -\hbar k/eB$. The k index is highly degenerate and is quantized according to the boundary conditions. The energy eigenvalues for F_{nk} are $E_n = (n - \frac{1}{2})\hbar\omega_c$, where $n = 1, 2, \dots$ and $\omega_c = e|B|/m_t$. We propose the following trial wavefunction, which includes the charge oscillations:

$$F_{xy}^{(nk)}(x', y') = f_{nk}(x', y') [1 + \alpha \cos(k_s x') + \beta \cos(2k_0\vartheta x')] / \sqrt{\Omega}. \quad (53)$$

Here, α and β are variational parameters and Ω is a normalization factor. The α and β terms reflect the modulations of the wavefunction due to commensurate and incommensurate charge oscillations, respectively. Numerically, we find that this trial function provides a good representation of the results from TB calculations. For simplicity, we consider the index $k = 0$ in Eqs. (52) and (53), corresponding to a Gaussian centered at $x' = 0$.

The total ground state energy ϵ is calculated using the trial wavefunction. In the $B \rightarrow 0$ limit, we obtain

$$\begin{aligned} \epsilon &= \epsilon^{(0)} - \epsilon_v + \epsilon_s \\ &= E_{\text{sb}} + \frac{(\hbar^2/m_t)(k_s^2\alpha^2/2 + 2k_0^2\vartheta^2\beta^2) - v_s\alpha - \bar{v}_v\beta}{2 + \alpha^2 + \beta^2}, \end{aligned} \quad (54)$$

where E_{sb} is the subband energy and we have defined $\bar{v}_v = v_v F_z^2(0)$.

In the limit of small \bar{v}_v , ϵ can be minimized by expanding $\alpha \simeq a_0 + a_1 \bar{v}_v^2$ and $\beta \simeq b \bar{v}_v$, collecting powers of \bar{v}_v , and minimizing them separately. The resulting valley coupling is given by

$$\epsilon_v = \frac{2\bar{v}_v^2 b}{2 + a_0^2}, \quad (55)$$

where

$$\begin{aligned} a_0 &= \left[-(\hbar^2 k_s^2/2m_t) + \sqrt{(\hbar^2 k_s^2/2m_t)^2 + 2v_s^2} \right] / v_s, \\ b^{-1} &= (\hbar^2/m_t)(2k_0^2\vartheta^2 - k_s^2/4) + \sqrt{(\hbar^2 k_s^2/4m_t)^2 + v_s^2/2}. \end{aligned}$$

For many experimental situations, including Ref. [6], the limit $v_s \ll \hbar^2 k_s^2/2m_t$ is appropriate, leading to

$\epsilon_v \simeq \bar{v}_v^2 m_t / 4\hbar^2 k_0^2 \vartheta^2$. We can use this result to obtain an estimate for the parameter \bar{v}_v in the experiments of Goswami, *et al.*⁶ In that system, the zero-field valley splitting was estimated be $E_v(0) = 2\epsilon_v = 1.5 \mu\text{eV}$, from which we obtain $\bar{v}_v \simeq 0.38 \text{ meV}$. This is tantalizingly close to the corresponding theoretical estimate, $\bar{v}_v = v_v F_z^2(0) = 0.36 \text{ meV}$, obtained using v_v from Eq. (28) and $F_z^2(0)$ from Eq. (46), with $\Delta E_c = 160 \text{ meV}$.

The emergence of incommensurate charge oscillations in the preceding analysis is a consequence of the fact that valley coupling breaks time reversal symmetry. However, the valley splitting in Eq. (55) is second order in the valley coupling parameter \bar{v}_v , since it results from a perturbation of the wavefunction (the charge oscillations). This explains why the experimental valley splitting is much smaller when $B = 0$ than when $B > 0$.⁶ In the $B > 0$ case, the valley splitting is first order in \bar{v}_v , since it arises from breaking the positional degeneracy of the magnetic eigenstates.⁴³ The smallness of the zero-field valley splitting may explain why it is not observed in Ref. [45].

IX. CONCLUSIONS

In this paper, we have developed an EM theory for the valley splitting in a strained SiGe/Si/SiGe quantum well by treating the valley coupling perturbatively. At zeroth order, we require a set of input parameters (the effective mass tensor) that can only be determined from a more microscopic theory, or from experiments. Similarly, at first order in the perturbation theory, we must input another parameter - the valley coupling constant v_v . The latter efficiently captures all the relevant, microscopic details of the interface, for the purposes of the EM theory. It is worth noting, however, that unlike bulk properties, the interface can vary from system to system, so that v_v should be determined for each case. In this work, we have used a two-band TB theory to compute v_v ,

as a function of the conduction band offset ΔE_c , assuming a sharp heterostructure interface. The results allow excellent agreement between the EM and TB theories.

Once v_v is known, we may apply the EM theory to a range of important problems. Here, we have considered the finite square well, with and without an applied electric field. We have also performed a self-consistent analysis of a 2DEG, using the Hartree approximation. Excellent agreement between EM and atomistic theories confirms our main conclusion, that the valley splitting in this system can be fully explained through a single coupling constant, v_v .

The EM theory is particularly useful for two or three-dimensional geometries, which cannot be easily treated in the TB approach, due to scaling limitations. We have applied the EM formalism to the important problem of valley splitting at zero magnetic field in a quantum well grown on a miscut substrate. In this case, we find a small (second order) valley splitting arising from spontaneous oscillations of the wavefunction. The quantitative results are in good agreement with experimental observations. At nonzero fields, the electronic wavefunctions are magnetically confined, producing an enhancement of the valley splitting, as described elsewhere.⁴³

N.B. In the final stages of preparation of this manuscript, we became aware of Ref. [46], which presents some similar results to those reported here.

Acknowledgments

We would like to acknowledge stimulating discussions with G. Klimeck, A. Punnoose, and P. von Allmen. This work was supported by NSA under ARO contract number W911NF-04-1-0389 and by the National Science Foundation through the ITR (DMR-0325634) and EMT (CCF-0523675) programs.

-
- ¹ P. Weitz, R. J. Haug, K. von Klitzing, and F. Schäffler, *Surf. Sci.* **361/362**, 542 (1996).
² S. J. Koester, K. Ismail, and J. O. Chu, *Semicond. Sci. Technol.* **12**, 384 (1997).
³ V. S. Khrapai, A. A. Shashkin, and V. P. Dolgoplov, *Phys. Rev. B* **67**, 113305 (2003).
⁴ K. Lai, *et al.*, *Phys. Rev. Lett.* **93**, 156805 (2004).
⁵ V. M. Pudalov, A. Punnoose, G. Brunthaler, A. Prinz, and G. Bauer, *cond-mat/0104347* (unpublished).
⁶ S. Goswami, *et al.*, *cond-mat/0408389* (unpublished).
⁷ M. A. Eriksson, *et al.*, *Quant. Inform. Process.* **3**, 133 (2004).
⁸ I. Zutic, J. Fabian, and S. Das Sarma, *Rev. Mod. Phys.* **76**, 323 (2004).
⁹ B. E. Kane, *Nature (London)* **393**, 133 (1998).
¹⁰ R. Vrijen, *et al.*, *Phys. Rev. A* **62**, 012306 (2000).
¹¹ M. Friesen, *et al.*, *Phys. Rev. B* **67**, 121301 (2003).
¹² W. Kohn, in *Solid State Physics*, edited by F. Seitz and D. Turnbull (Academic Press, New York, 1957), Vol. 5.
¹³ T. Ando, A. B. Fowler, and F. Stern, *Rev. Mod. Phys.* **54**, 437 (1982).
¹⁴ P. Y. Yu and M. Cardona, in *Fundamentals of Semiconductors*, Third Edition (Springer-Verlag, Berlin, 2001).
¹⁵ S. T. Pantelides and C. T. Sah, *Phys. Rev. B* **10**, 621 (1974).
¹⁶ M. Friesen, *Phys. Rev. Lett.* **94**, 186403 (2005).
¹⁷ T. B. Boykin, *et al.*, *Appl. Phys. Lett.* **84**, 115 (2004).
¹⁸ T. B. Boykin, *et al.*, *Phys. Rev. B* **70**, 165325 (2004).
¹⁹ T. B. Boykin, G. Klimeck, P. von Allmen, S. Lee, and F. Oyafuso, *Journ. of Appl. Phys.* **97**, 113702 (2005).
²⁰ F. J. Ohkawa and Y. Uemura, *J. Phys. Soc. Japan* **43**, 907 (1977).
²¹ F. J. Ohkawa and Y. Uemura, *J. Phys. Soc. Japan* **43**, 917 (1977).
²² F. J. Ohkawa, *Solid State Commun.* **26**, 69 (1978).
²³ L. J. Sham and M. Nakayama, *Phys. Rev. B* **20**, 734

- (1979).
- ²⁴ T. Ando, A. B. Fowler, and F. Stern, *Rev. Mod. Phys.* **54**, 437 (1982).
- ²⁵ F. J. Ohkawa, *J. Phys. Soc. Japan* **46**, 736 (1979).
- ²⁶ T. Ando, *Phys. Rev. B* **19**, 3089 (1979).
- ²⁷ J. H. Davies, *The Physics of Low-Dimensional Semiconductors* (Cambridge Press, Cambridge, 1998).
- ²⁸ F. Long, W. E. Hagston, and P. Harrison, in *23rd International Conference on the Physics of Semiconductors*, edited by M. Sheffler and R. Zimmermann (World Scientific, Singapore, 1996) p. 819.
- ²⁹ C. Herring and E. Vogt, *Phys. Rev.* **101**, 944 (1956).
- ³⁰ F. Schäffler, *Semicond. Sci. Technol.* **12**, 1515 (1997).
- ³¹ B. Koiller, X. Hu, and S. Das Sarma, *Phys. Rev. B* **66**, 115201 (2002).
- ³² H. Fritzsche, *Phys. Rev.* **125**, 1560 (1962).
- ³³ W. D. Twose, in the Appendix of Ref. [32].
- ³⁴ B. A. Foreman, *Phys. Rev. B* **72**, 165345 (2005).
- ³⁵ K. Shindo and H. Nara, *J. Phys. Soc. Japan* **40**, 1640 (1976).
- ³⁶ X. Hu, B. Koiler, and S. Das Sarma, *Phys. Rev. B* **71**, 235332 (2005).
- ³⁷ C. J. Wellard, *et al.*, *Phys. Rev. B* **68**, 195209 (2003).
- ³⁸ C. J. Wellard and L. C. L. Hollenberg, *Phys. Rev. B* **72**, 085202 (2005).
- ³⁹ L. C. L. Hollenberg, C. J. Wellard, and A. D. Greentree, unpublished.
- ⁴⁰ M. Nakayama and L. J. Sham, *Solid State Commun.* **28**, 393 (1978).
- ⁴¹ K. Takashina, Y. Ono, A. Fujiwara, Y. Takahashi, and Y. Hirayama, *Phys. Rev. Lett.* **96**, 236801 (2006).
- ⁴² M. M. Roberts, *et al.*, *Nature Mater.* **5**, 388 (2006).
- ⁴³ M. Friesen, M. A. Eriksson, and S. N. Coppersmith, cond-mat/0602194 (unpublished).
- ⁴⁴ For a quantum well tilted with respect to the crystallographic axes, the effective mass tensor is not fully diagonal. There is an off-diagonal term $m_{xz}^{-1} \simeq \theta(m_t^{-1} - m_l^{-1})$, where m_t and m_l are the transverse and longitudinal effective masses. For a 2° miscut, we find $m_t/m_{xz} = 0.028$. The off-diagonal corrections can then be included perturbatively. Here, we consider only the leading order (diagonal) mass terms.
- ⁴⁵ P. von Allmen and S. Lee, cond-mat/0606395 (unpublished).
- ⁴⁶ M.O. Nestoklon, L.E. Golub, and E.L. Ivchenko, cond-mat/0601520 (unpublished).